Landslides and Engineered Slopes: Protecting Society through Improved Understanding – Eberhardt et al. (eds)

Modeling of propagation and entrainment phenomena for landslides of the flow type: The May 1998 case study

L. Cascini & S. Cuomo
University of Salerno, Italy

M. Pastor
Universidad Politecnica de Madrid, Spain

G. Sorbino & L. Piciullo
University of Salerno, Italy

ABSTRACT: Rainfall-induced landslides of the flow type are dangerous phenomena due to their high velocities and large run-out distances. Indeed, proper modeling of their propagation stage is a fundamental issue for risk analysis and management. To this aim, several factors must be taken into account to properly estimate the run-out distance and the landslide magnitude that are strongly related to an appropriate choice of the rheological properties of the moving mass. Moreover, several distinct processes must be adequately tackled such as: i) relative movement of the interstitial fluid relative to the solid fraction, ii) vertical consolidation process, iii) entrainment of material along the landslide path. All the above mentioned processes can be consistently simulated through the use of a depth-integrated coupled SPH model which revealed to be appropriate in simulating landslides of the flow type. In this paper, taking into account the entrainment phenomena, the above model is applied to the May 1998 Sarno-Quindici case history (Southern Italy) for which an advanced data-set is available. The numerical analyses provide a satisfactory simulation of the observed propagation path, deposition heights and velocities that are strongly influenced by the entrainment rate and the extent of the erodible area.

1 INTRODUCTION

Landslides of the flow type are catastrophic events that may occur all over the world even resulting in great number of casualties and widespread damages.

In fact, these landslides travel at extremely high velocities (in the order of meters/second) and can impact large areas, also far from their source (up to tens of kilometers), arriving to piedmont areas which are often settled due to more favorable conditions for urban development.

Indeed, the prediction of both run-out distances and velocities during the propagation stage can notably reduce losses inferred by these phenomena, as it provides a means for: i) defining the hazardous areas, estimating the intensity of the hazard (which serves as input in risk studies) and ii) working out the information for the identification and design of appropriate mitigation strategies (Fell et al., 2008).

To this aim, one more important issue, not often taken into account in the propagation models, is the entrainment of material along the propagation path which may greatly modify the landslide volume and velocity that define the intensity of the event.

For the analysis (and forecast) of the entrainment phenomena, several approaches are available, most of them are empirical while very few are analytical (e.g., Medina et al., 2008). For instance, Hungr (1995) simply relates the increase of landslide volume to the run-out distance. Conversely, in the most advanced approaches the amount of entrained material is related to the computed height and velocity of the propagating mass through mathematical models.

Among these last, the depth-integrated coupled models in combination with the SPH numerical method provide an attractive framework for flow-like landslides modelling. This is essentially related to the calculation time that is low compared to classical, Eulerian finite elements, as the computational grid is separated from the structured terrain mesh used to describe terrain topography.

The depth integrated coupled SPH model proposed by Pastor (2007, 2009) is also able to take into account pore water pressures dissipation in the

propagating mass (Pastor et al., 2002, 2004) and its potentiality was assessed using either benchmarks or applications to case histories (Pastor et al., 2007, 2009).

Considering that the assessment of the erodible areas as well as the estimation of the erosion rates are still challenging topics, a case history from Southern Italy, for which an extensive geotechnical data-set is available, is analyzed in the paper. Particularly, the above SPH model is applied referring to the entrainment formula proposed by Hungr (1995).

2 CASE STUDY

2.1 *May 1998 Sarno-Quindici landslides*

Landslides of the flow type frequently cause victims and huge economic damages when they involve the pyroclastic soils (Bilotta et al., 2005) originated by the explosive activity of Somma-Vesuvius volcano (Campania region—Southern Italy) which cover a carbonate bedrock over an area 1,400 km^2 large.

The most catastrophic recent natural disaster occurred on 4–5 May 1998 (Fig. 1). During this event, more than a hundred slope instability phenomena affected the slopes of the Pizzo d'Alvano massif; tens of flow-type landslides travelled up to the towns of Bracigliano, Quindici, Sarno and Siano located at the toe of the massif (Cascini 2004, Cascini et al., 2008, Guadagno et al., 2005). Globally, 2 million cubic meters of soil/material were mobilized which caused 159 victims and 500 million Euros of damages to buildings and infrastructures (Cascini 2004).

Flow-type landslides occurred in almost all the mountain basins of the massif and their source areas were primarily located at the upper parts of the hillslopes. For these events, six triggering mechanisms were individuated which caused distinct landslide volumes and run-out distances (Cascini et al., 2008, 2011).

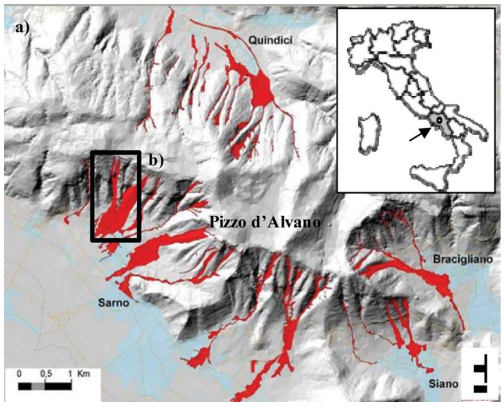

Figure 1. Overview of the 1998 Pizzo d'Alvano landslides (a) and location of the selected basin (b).

As landslides travelled down-slope, their initial volume increased due to: i) soil erosion in the gullies below and ii) incorporation, in some cases, of minor slides mobilized along the flanks of the gullies (Cascini 2004). It is worth noting that entrainment phenomena amplified the triggered volumes by a factor of 1.5 for the largest landslides (Cascini et al., 2006).

In the scientific literature, direct measurements are not available for the landslide velocities while they were indirectly estimated. Faella & Nigro (2003), based on the analysis of the observed damages to the buildings due to the landslide impact, indicate values of 3–20 m/s in the piedmont areas. Revellino et al. (2004), by measuring the flow super-elevation in the channel bends, provide a typical velocity range of 5–15 m/s.

2.2 *Literature review on the propagation stage*

Due to their consequences, many other aspects of the propagation stage of the May 1998 landslides event are extensively analyzed in the literature.

Most of the contributions focuses on the geometrical characteristics of the landslides. Particularly, heuristic methods are applied by Pareschi et al. (2002) and Budetta & de Riso (2004) who analyze the height of fall (H) and run-out distance (L) of the landslides. In both contributions, the above quantities are computed between the uppermost landslide source area and the lowest deposition zone (along the propagation path) and they are related by linear functions.

As a further contribution, Di Crescenzo & Santo (2005) outline that the height of fall is also strongly related to the length of the deposition zone.

Differentiating the landslides based on slope morphology, landslide source areas and presence of anthropogenic structures, Cascini et al. (2011) highlight that: i) the source areas location affected the landslide reach angle (ratio of H to L) with higher values computed in the northwest sector of the massif (i.e., Quindici and Bracigliano) and lower in the southern sectors of the massif (i.e., Sarno and Siano), ii) the triggering mechanism and the features of the associated source areas influenced the propagation stage in terms of either reach angles or travel distances, iii) multiple landslides (i.e., landslides which joined along the propagation path) had longer travel distances and lower reach angles and finally iv) anthropogenic structures, such as paved roads and channels

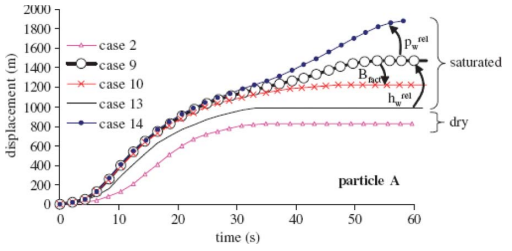

Figure 2. Displacement-time curves simulated for a particle triggered in the landslide source area (Pastor et al., 2009).

located at the toe of hillslopes, significantly increased the landslide run-out.

The above heuristic approaches while providing an overall understanding of the landslide mobility do not allow analyzing their kinematic features (e.g., velocity and height) for which the current literature provides some contributions through the mathematical modelling.

For instance, Pastor et al. (2009) using a depth-integrated mathematical model and disregarding the entrainment phenomena show that both landslide run-out distance and velocity are strongly affected by pore water pressures and, in particular, by the: i) initial pore water pressure $\left(p_w^{rel}\right)$, ii) initial height of the water table $\left(h_w^{rel}\right)$ and iii) vertical consolidation coefficient (B_{fact}) (Fig. 2). Using this model a satisfactory back-analysis of the events is also provided by the Authors.

Vice versa, Revellino et al. (2004) disregarding the pore pressure and by applying the 1D mathematical model proposed by Hungr (1995), emphasize the role of entrainment in both landslide source and propagation areas. In particular, entrainment is assessed capable to increase the initial volumes by a factor of 30 for the largest landslides.

In conclusion, the current literature while providing several insights on the selected case study does not still allow to properly understand the role of entrainment during the propagation stage. A contribution to the topic is hereafter proposed based on a mathematical modeling of two important landslides performed through the above mentioned depth-integrated coupled SPH model (Pastor et al., 2009).

3 NUMERICAL MODELLING

3.1 *Mathematical model*

In the theoretical framework, mainly derived by the contributions of Hutchinson (1986) and Pastor et al. (2002, 2004), the propagating mass is schematized as a mixture of a solid skeleton saturated with water and the unknowns are the velocity of the solid skeleton (v) and the pore water pressure (p_w).

For the propagation stage of landslides, the governing equations are the following: i) the balance of mass of the mixture combined with the balance of linear momentum of the pore fluid, ii) the balance of linear momentum of the mixture, iii) the rheological equation relating the soil stress tensor to the rate of deformation tensor and iv) the kinematical relations between the rate of deformation tensor to the velocity field. From here, a propagation–consolidation model is derived assuming that pore pressure dissipation takes place along the normal to the terrain surface, assuming that the velocity of solid skeleton and pressure fields can be split into two components, i.e., propagation and consolidation as $v = v_0 + v_1$ and $p_w = p_{w0} + p_{w1}$. Since many flow-like landslides have average depths small in comparison with their length or width, the above equations can be integrated along the vertical axis and the resulting 2D depth integrated model presents an excellent combination of accuracy and simplicity.

With reference to the numerical discretization, the Smoothed Particle Hydrodynamics (SPH) method is used. As in any meshless method, the propagating mass is schematized through a set of moving "particles" or "nodes" to which information concerning field variables and their derivatives is linked. Of course, the level of approximation depends on how the nodes are spaced and on their location. Based on this numerical discretization, the depth-integrated coupled SPH model consists on a set of ordinary differential equations whose details are provided by Pastor et al. (2009).

In this model, material entrainment causes the elevation decrease of the ground surface in time depending on: i) height of propagating mass, ii) velocity and iii) entrainment rate. The latter is hereafter computed according to Hungr (1995) and assumed as an input in the analyses. The entrained material is assumed to have nil velocity and nil pore water pressure when included in the propagating mass.

3.2 *Input and methods*

The modeling of either propagation and entrainment is performed for a selected basin (Figs. 1b, 3) where two landslide source areas were triggered at an altitude of 500–700 m a.s.l. with a total mobilized volume of about 50,000 m^3 (Cascini et al., 2006). Particularly, triggered masses joined in a channel with steep flanks. There the whole mass

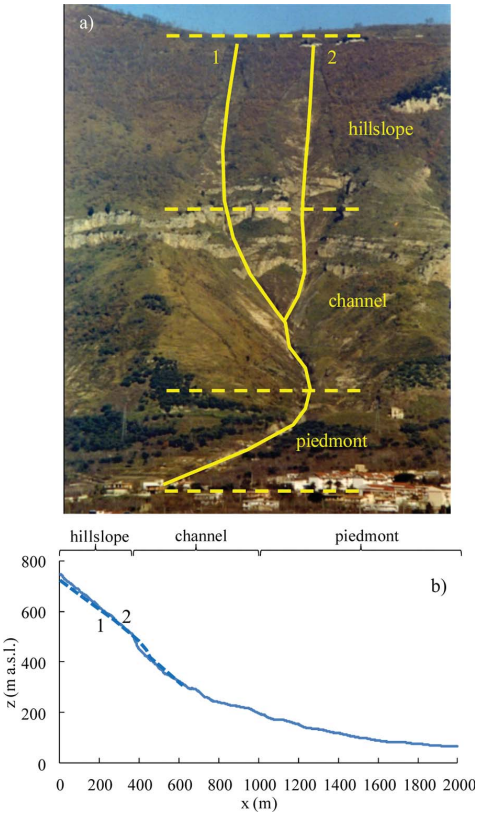

Figure 3. Overview of the "Tuostolo" mountain basin and 1998 landslides (a), longitudinal slope profile (b).

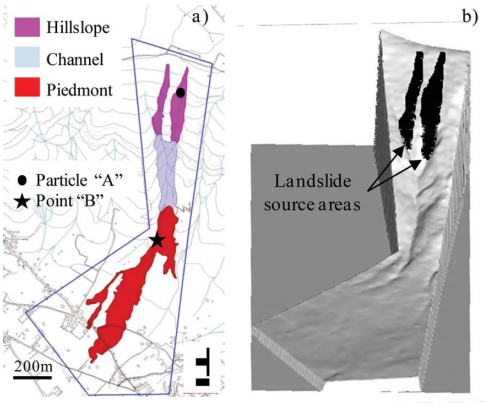

Figure 4. Morphological zoning of 1998 landslides (a), 3D view of the 5 m × 5 m Digital Elevation Model used for the numerical analyses (b).

travelled about 1500 meters of which 400 meters in the channel and 1100 meters in a flatter piedmont area (Fig. 4a).

As input for the SPH model, a 5 m × 5 m Digital Elevation Model was used which well reproduces the pre-event conditions (Fig. 4b). As for the temporal discretization of the analysed process, an automatic adaptive time stepping (Pastor et al., 2002) was used with time intervals shorter than 0.8 s.

The frictional rheological model was referred and its properties selected also based on those used by Pastor et al. (2009)—case 0 in Table 1—who do not consider any erodible area for their analysis. Instead, in this paper different hypotheses are considered for the: i) erodible area "A_{er}" corresponding to either the channel, piedmont or both and ii) erosion rate "Er" whose values are reported in Table 1. Particularly, the minimum and maximum erosion rates ($4.0 \times 10^{-4} \div 1.3 \times 10^{-3}$ m^{-1}) were estimated applying the empirical relation of Hungr (1995) to the travel distances, initial and final volumes of the May 1998 landslides.

3.3 *Numerical results*

It must first be observed that the material entrainment in the channel (Table 1, case 1) or along the entire propagation path, i.e., channel and piedmont (Table 1, case 2), greatly modifies the landslide propagation pattern. In the former case (Fig. 5), the simulated landslide travels more along the right-hand side; in the latter case (Fig. 6), the material entrainment at the hillslope piedmont prevents the landslide propagation along the right side and, in turn, causes a longer propagation along the left side. In the above cases, despite a distinct propagation area, the simulated run-out distances are similar but shorter than that observed. Moreover, assuming the maximum estimated erosion rate (Table 1, case 3), the landslide completely stops at the end of the channel where a thick deposit develops (Fig. 7).

The above results mismatch the in-situ evidences while a satisfactory simulation is obtained for

Table 1. Rheological soil parameters assumed for the numerical simulations.

Case #	tanφ' (–)	h^{rel}_w (–)	p^{rel}_w (–)	B_{fact} (m^2 s^{-1})	Er (m^{-1}) channel	Er (m^{-1}) piedmont
0*	0.4	0.25	1.0	1.1×10^{-2}	0	0
1	0.4	0.25	1.0	1.1×10^{-2}	4.0×10^{-4}	0
2	0.4	0.25	1.0	1.1×10^{-2}	4.0×10^{-4}	4.0×10^{-4}
3	0.4	0.25	1.0	1.1×10^{-2}	1.3×10^{-3}	1.3×10^{-3}
4	0.4	0.4	1.0	1.0×10^{-2}	4.0×10^{-4}	0

φ': friction angle, h^{rel}_w: relative water height, p^{rel}_w: relative pore water pressure, B_{fact}: consolidation factor, Er: erosion rate. (*) values assumed in Pastor et al. (2009).

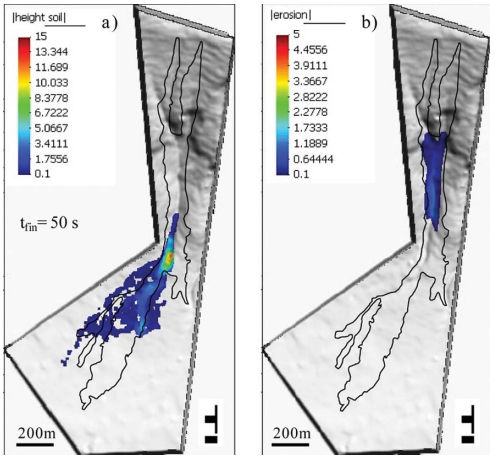

Figure 5. Heights of the propagating mass (a) and eroded heights (b) computed assuming the minimum erosion rate in the channel (case 1 of Table 1).

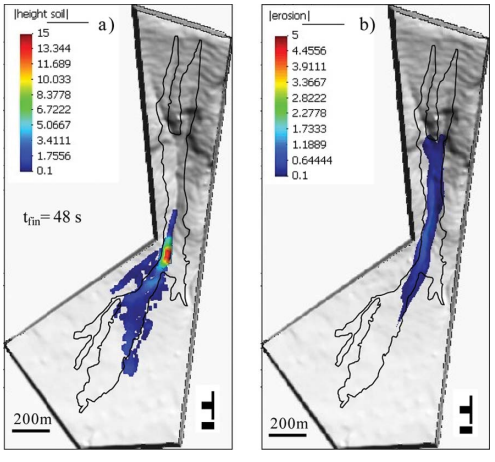

Figure 6. Heights of the propagating mass (a) and eroded heights (b) computed assuming the minimum erosion rate in both the channel and piedmont area (case 2 of Table 1).

case 4 of Tab. 1 that allows to well interpret both the run-out distance and extent of propagation-deposition zones (Fig. 8). Minor mismatches are instead related to the complex morphology of the landslide deposit which could have been influenced by either partial deposition of the first propagating mass or diversion of the following volumes.

Quantitative comparisons among the above cases are reported in Figure 9 which shows the velocities and heights computed for the particle "A" of Figure 4 initially located in the landslide source area.

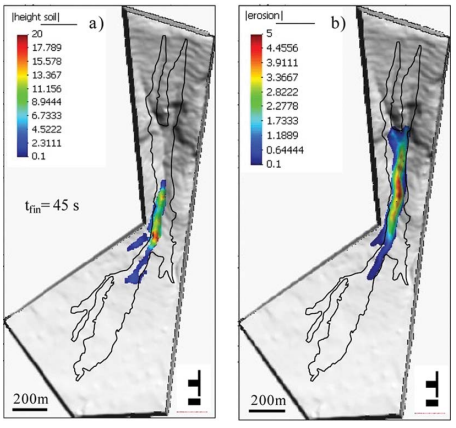

Figure 7. Heights of the propagating mass (a) and eroded heights (b) computed assuming the maximum erosion rate in both the channel and piedmont area (case 3 of Table 1).

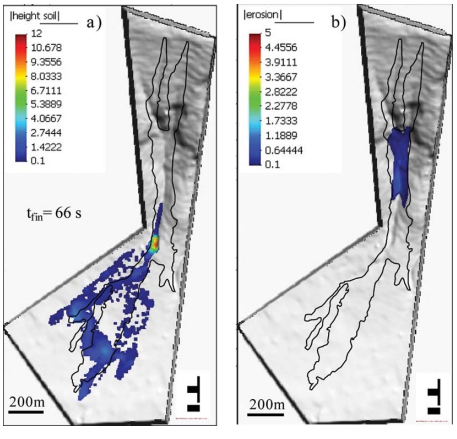

Figure 8. Best simulation of the in-situ evidences (case 4 of Table 1).

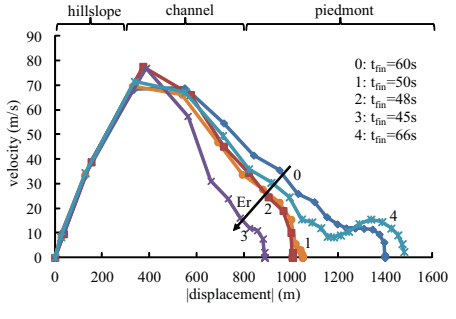

Figure 9. Simulated velocity and displacement for the particle A of figure 4 with the indication of the zones (hillslope, channel and piedmont) of the Tuostolo basin.

For instance, in the hillslope and in the uppermost channel, the displacement-velocities curves coincide in all the cases because the kinematical features of the propagating mass are mainly related to: i) the volume mobilized in the source area and ii) topography which are the same in all the simulations.

As the unstable mass propagates downslope the effects of the erosion phenomena appear more relevant. Particularly, the entrained material brakes the landslide along distinct propagation paths also depending on soil deposition patterns at the hillslope piedmont (cases 0, 2 and 3). In the Figure 9, it can be also noted that cases 0 and 4 globally almost coincide; however, some important differences are outlined in the channel and piedmont zones where the case 4 outlines higher velocities of the propagating mass and higher heights of the landslide deposit.

Another comparison is provided in terms of computed heights at the point "B" of Figure 4 which is representative of the overall landslide propagation-deposition stage (Fig. 10). Particularly, an increasing erosion rate (Er) causes the height-time curves change with a smoother peak (respectively case 0, 2 and 3); the latter corresponds to the arrival of two following masses at the considered point. At the same location, the final simulated heights increase with Er because deposition occurs rather than propagation. In the same plot, it is also shown that: i) the propagation path and deposition stage depend on the extent of the erodible areas (A_{er}), ii) disregarding the entrainment phenomena an underestimation of the deposition heights can be obtained especially at the end of the channel (case 0 instead of case 4).

It is worth noting that material entrainment while significantly modifying the landslide propagation path does not much affect the duration of the wholepropagation-deposition stage (45 to 66 seconds for cases 0–4). Comparison of the results obtained for cases 0, 1 and 4 shows that a fundamental role towards the landslide mobility assessment is always played by the initial height of the water table $\left(h_w^{rel}\right)$.

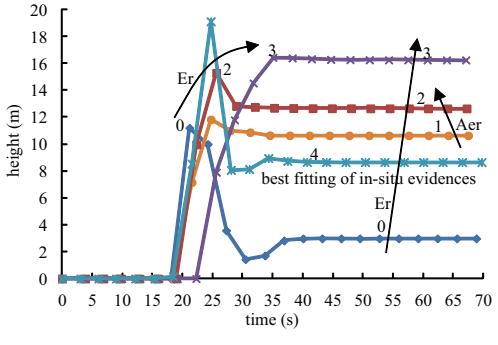

Figure 10. Simulated heights at the point "B" of Figure 4.

4 CONCLUDING REMARKS

In the paper a depth-integrated coupled SPH model is applied for the simulation of landslides of the flow type by considering either pore water pressures consolidation or material entrainment along the propagation path. Apart from a satisfactory back-analysis of the selected case history, some general insights are provided by the numerical results: i) the run-out distance globally diminishes as the erosion rate increases (in the channel or at piedmont area), ii) entrainment may cause different landslide propagation paths, iii) erosion phenomena play a major role for landslide propagation run-out when they affect areas characterized by high velocities and heights (typically in the channel areas), iv) an adequate modeling of the run-out distance can be obtained by either neglecting or including the entrainment phenomena if the rheological parameters are well calibrated. From a technical point of view, if entrainment phenomena may occur, they must be taken into account to properly evaluate the landslide deposition heights in the piedmont zones. To this aim, a key factor for the numerical modeling is represented by the initial height of the water table in the source areas.

REFERENCES

Bilotta, E., Cascini, L., Foresta, V. & Sorbino, G. 2005. Geotechnical characterization of pyroclastic soils involved in huge flowslides. *Geotech. and Geol. Eng.* 23:365–402.

Budetta, P. & de Riso, R. 2004. The mobility of some debris flows in pyroclastic deposits of the northwestern Campanian region southern Italy. *Bull Eng Geol Environ* 63:293–302.

Cascini, L. 2004. The flowslides of May 1998 in the Campania region, Italy: the scientific emergency management. *Italian Geotechnical Journal* 2:11–44.

Cascini, L., Cuomo, S. & Della Sala, M. 2011. Spatial and temporal occurrence of rainfall-induced shallow landslides of flow type: A case of Sarno-Quindici, Italy. *Geomorphology* 126(1–2):148–158.

Cascini, L., Cuomo, S. & Guida, D. 2008. Typical source areas of May 1998 flow-like mass movements in the Campania region, Southern Italy. *Engineering Geology* 96:107–125.

Cascini, L., Guida, D. & Sorbino, G. 2006. Il Presidio Territoriale: una esperienza sul campo. *G.N.D.C.I.-C.N.R. Edition*, p. 139.

Di Crescenzo, G. & Santo, A. 2005. Debris slides-rapid earth flows in the carbonate massifs of the Campania region Southern Italy): morphological and morphometric data for evaluating triggering susceptibility. *Geomorphology* 66:255–276.

Faella, C. & Nigro, E. 2003. Dynamic impact of the debris flows on the constructions during the hydrogeological disaster in Campania 1998: failure mechanical models and evaluation of the impact velocity. *Prediction and Prevention for Risk Mitigation*, *Proc. Int. Conf. on Fast Slope Movements, Napoli*, pp. 179–186.

Fell, R., Corominas, J., Bonnard, Ch., Cascini, L., Leroi, E. & Savage. W.Z. 2008. Guidelines for landslide susceptibility, hazard and risk zoning for land use planning. *Joint Technical Committee on Landslides and Engineered Slopes Engineering Geology* 102:85–98.

Guadagno, F.M., Forte, R., Revellino, P., Fiorillo, F. & Focareta, M. 2005. Some aspects of the initiation of debris avalanches in the Campania Region: the role of morphological slope discontinuities and the development of failure. *Geomorphology* 66:237–254.

Hungr, O. 1995. A model for the run-out analysis of rapid flow slides, debris flows and avalanches. *Canadian Geotechnical Journal* 32:610–623.

Hutchinson, J.N. 1986. A sliding-consolidation model for flow slides. *Canadian Geotechnical Journal*; 23:115–126.

Medina, V., Hurlimann M. & Bateman, A. 2008. Application of FLATModel, a 2D finite volume code, to debris flows in the northeastern part of the Iberian Peninsula. *Landslides 5(1)*:127–142.

Pareschi, M.T., Santacroce, R., Sulpizio, R. & Zanchetta, G. 2002. Volcaniclastic debris flows in the Clanio Valley (Campania, Italy): insights for the assessment of hazard potential. *Geomorphology* 43:219–231.

Pastor, M., Blanc, T., Pastor, M.J., Sanchez, M., Haddad, B., Mira, P., Fernandez Merodo, J.A., Herreros, M.I. & Drempetic, V. 2007. A SPH depth integrated model with pore pressure coupling for fast landslides and related phenomena. In Ho & Li (eds.), *2007 International Forum on Landslides Disaster Management*.

Pastor, M., Haddad, B., Sorbino, G., Cuomo, S. & Drempetic, V. 2009. A depth-integrated, coupled SPH model for flow-like landslides and related phenomena. *Int. J. Numer. Anal. Meth. Geomech* 33:143–172.

Pastor, M., Quecedo, M., Fernandez-Merodo, J.A., Herreros, M.I., Gonzalez, E. & Mira, P. 2002. Modelling tailing dams and mine waste dumps failures. *Geotechnique* 52:579–591.

Pastor, M., Quecedo, M., Gonzalez, E., Herreros, M.I., Fernandez Merodo, J.A. & Mira, P. 2004. Modelling of landslides (II) propagation. In *Degradation and Instabilities in Geomaterials*. Springer: New York, pp. 319–367.

Revellino, P., Hungr, O., Guadagno, F.M. & Evans, S. 2004. Velocity and run-out simulation of destructive debris flows and debris avalanches in pyroclastic deposits, Campania region, Italy. *Environmental Geology* 45:295–311.